

# 1 Response to Editor Review of Dr. Klaus Gierens (21 Mar 2016)

Thank you very much for your time. All your corrections are greatly appreciated and surely improved the clarity and readability of the manuscript. Also, please find a differential version of the manuscript at the end of response section.

## 1.1 General remarks

- *I have one major comment, similar to the major comment of referee #1, but potentially in another direction. This is the following point: Lines 290 to 319: As I see it, the choice of the RT solver or spectral integration scheme has only a minor impact on simulated cloud properties. A better way to compare the differences would be to run the same simulation with a slightly different realization of the initial temperature field (superposed with some noise). This would lead to variations relative to the original simulation as well and would provide a basis to judge whether a difference caused by different RT methods in within or without the noise. How is the effect on radiation quantities like  $\text{div } F$ ?*

Good point, we repeated a calculation with full spectral integration and a random temperature perturbation. The temperature perturbation introduces differences comparable in magnitude to the ones from Monte-Carlo-Spectral-Integration. Under the assumption that with  $\text{div } F$  you mean the flux divergence i.e. the heating rates — we find it difficult to interpret radiation quantities advantageously due to the tremendous noise that is introduced by the Monte-Carlo-Spectral-Integration (uniform and original). However, to point out one particular reassuring fact: integrated over the period of the simulations, the uniform as well as the original Monte-Carlo-Spectral-Integration remain unbiased with respect to heating rates.

## 1.2 Specific comments

- *Line 38/39: Explain “atmospheric aggregation”*  
Done.
- *Lines 44–47: how can model errors affect cloud formation? Please rewrite.*

We added two sentences to further illustrate cloud-radiative feedbacks.

- *Lines 50–53: Please rewrite this as well. As it stands, it is the coupling that is expensive. But it is the execution of an LES coupled to 3D radiative transfer that is expensive.*

Yes, done.

- *Line 62: The logic of your argumentation would be clearer with “even more expensive LBL calculations”.*

Done.

- *Line 78: The error is uncorrelated to what? And what does “The error is statistical” mean?*

Fixed, thanks.

- *Line 85: please rewrite “. . . not meaningful to calculate a spectral band in one column and a different band in a neighbouring column.”*

Done.

- *Lines 166–169: please rewrite. As it stands, the coupling is solved instead of the equation system.*

Done.

- *Line 171: The expansion of PETSc should be moved from ll 189/90 to here where it appears first.*

Done.

- *Lines 183–185: An equation system can not be written as one matrix. A matrix is not an equation. Please rewrite.*

Done.

- *Line 197: More efficient than what? Line 198: easier than what?*

Indeed, we removed the sentence altogether as it is not relevant for our work. We are after all not writing novel iterative solvers.

- *Line 227: What is a sparsity pattern? Please reformulate.*

Done.

- *Lines 239/240: There is a break of logic between the last sentence and the discussion before. The last sentence should be moved to a more appropriate place.*

Moved to the end of the section.

- *Line 244: the notion “high frequency error” needs some explanation. The corresponding “low frequency error” should then be a clear notion as well. About which errors are you talking here?*

Rewrote the two sentences to clarify. Changed the wording from error to residual to clarify that we are talking about intermediate residuals during the matrix solver iterations.

- *Line 277: Again, “the error is uncorrelated”. To what?*

We added “... uncorrelated in space and time.”

- *Lines 283–289: Try to rewrite these sentences. For instance: “It is not clear whether the assumptions ... when we reduce the sampling noise. We repeated ... in order to test this.”*

Done.

- *Caption of figure 2, last sentence: Is it possible to describe the meaning of the grey bar without “alpha channel”. Probably many users don’t know what this is, and to my opinion it is not really needed.*

Indeed, we just removed the “alpha channel” keyword.

Many thanks,

Fabian Jakob

# 3D Radiative Transfer in Large-Eddy Simulations – Experiences coupling the TenStream solver to the UCLA–LES

Fabian Jakub<sup>1</sup> and Bernhard Mayer<sup>1</sup>

<sup>1</sup>LMU Munich, Theresienstr.37 80333 Munich

Correspondence to: Fabian Jakub (fabian.jakub@physik.uni-muenchen.de)

**Abstract.** The recently developed three dimensional Ten-Stream radiative transfer solver was integrated into the UCLA–LES cloud resolving model. This work documents the overall performance of the TenStream solver as well as the technical challenges migrating from 1D schemes to 3D schemes. In particular the employed Monte-Carlo-Spectral-Integration needed to be re-examined in conjunction with 3D radiative transfer. Despite the fact that the spectral sampling has to be performed uniformly over the whole domain, we find that the Monte-Carlo-Spectral-Integration remains valid. To understand the performance characteristics of the coupled TenStream solver, we conducted weak- as well as strong-scaling experiments. In this context, we investigate two matrix-preconditioner (GAMG and block-jacobi ILU) and find that algebraic multigrid preconditioning performs well for complex scenes and highly parallelized simulations. The TenStream solver is tested for up to 4096 cores and shows a parallel scaling efficiency of 80 % to 90 % on various supercomputers. Compared to the widely employed 1D  $\delta$ -Eddington two-stream solver, the computational costs for the radiative transfer solver alone increases by a factor of five to ten.

## 1 Introduction

To improve climate predictions and weather forecasts we need to understand the delicate linkage between clouds and radiation. A trusted tool to further our understanding in atmospheric science is the class of models known as large-eddy-simulations (LES). These models are capable of resolving the most energetic eddies and were successfully used to study boundary layer structure as well as shallow and deep convective systems.

Radiative heating and cooling drives convective motion and influences cloud droplet growth and micro-

physics (Harrington et al., 2000; Marquis and Harrington, 2005). Recent work suggests that cloud radiative feedbacks may also play an important role in atmospheric aggregation convective self-aggregation, i.e. how clouds are organized in the atmosphere (Muller and Bony, 2015). One aspect that has, until now, been studied only briefly is the role of three dimensional radiative transfer. One dimensional radiative transfer by definition ignores effects such as cloud side illumination, displaced cloud shadows and horizontal energy transport in general. While it is clear that the neglect of these three dimensional effects lead to big errors in heating rates, the question if and how much this has these have an effect on cloud formation is not yet settled (Schumann et al., 2002; Di Giuseppe and Tompkins, 2003; O’Hirok and Gautier, 2005; Frame et al., 2009; Petters, 2009). Particular cloud-radiative feedbacks are for example, an increased sensible and latent heat flux in the updraft region caused by displaced cloud shadows or the immediate change of the flow through non-adiabatic radiative heating or cooling.

While radiative transfer is probably the best understood physical process in atmospheric models it is extraordinarily expensive (computationally) to couple-use fully three dimensional radiative transfer solvers to-in LES models.

One reason for the computational complexity involved in radiative transfer calculations is the fact that solvers are not only called once per time step but the radiative transfer has to be integrated over the solar and thermal spectral ranges. A canonical approach for the spectral integration are so called “correlated-k” approximations (Fu and Liou, 1992; Mlawer et al., 1997) where instead of even more expensive line-by-line calculations, the spectral integration is done with typically one to two hundred spectral bands.

However, even when using simplistic 1D radiative transfer solvers and correlated-k methods for the spectral integration the computation of radiative heating rates is very demanding.

As a consequence, radiation is usually not calculated at each time step but rather updated infrequently. This is problematic, in particular in the presence of rapidly changing clouds. Further strategies are needed to render the radiative transfer calculations computationally feasible.

One such strategy was proposed by Pincus and Stevens (2009) who state that thinning out the calling frequency temporally is equivalent to a sparse sampling of spectral intervals. They proposed not to calculate all spectral bands at each and every time step but rather to pick one spectral band randomly. The error that is introduced by the random sampling is assumed to be ~~statistical and uncorrelated and unbiased~~ and uncorrelated in space and time and should not change the overall course of the simulation. Their algorithm is known as Monte-Carlo-Spectral-Integration and is implemented in the UCLA-LES. For each time step and for each vertical column, a spectral band is chosen randomly. This has important consequences for the application of a 3D solver where every column is coupled to its neighbors ~~and it is not meaningful to calculate a different~~. Calculating a particular spectral band in one column and ~~another at a different one in the neighboring column~~ -would erroneously imply that the light changes its frequency going from column to column. Instead, in the case of a 3D solver, we need to use one spectral band for the entire domain. Hence, in order to couple the TenStream solver to the UCLA-LES we need to revisit the Monte-Carlo-Spectral-Integration and check if it is still valid if used with three dimensional solvers.

Another reason for the computational burden is the complexity of the radiation solver alone. Fully three-dimensional solvers such as MonteCarlo (Mayer, 2009) or SHDOM (Evans, 1998) are several orders of magnitude slower than usually employed 1D solvers (e.g.  $\delta$ -Eddington two-stream (Joseph et al., 1976)).

To that end, there is still considerable effort being put into the development of fast parameterizations to account for 3D effects. Recent works incorporate 3D effects in low resolution sub-grid-cloud aware models (GCM's) by means of overlap assumptions or additional horizontal exchange coefficients (Tompkins and Di Giuseppe, 2007; Hogan and Shonk, 2013). Other parameterizations target high resolution models and propagate radiation on the grid-scale, e.g. Frame et al. (2009) or Wissmeier et al. (2013) for the solar spectral range or Klinger and Mayer (2015) for the thermal.

The TenStream solver (Jakub and Mayer, 2015) is a rigorous, fully coupled, three-dimensional, parallel and, comparably fast radiative transfer approximation. In brief, given the optical properties in a box (absorption and scattering coefficient as well as the asymmetry parameter), the TenStream solver computes the propagation of radiation for each model box using MonteCarlo techniques and stores the respective transport coefficients in a look-up table. The resulting radiative fluxes of one box are then coupled in the vertical (2 streams) as well as in the horizontal directions (8 streams) with their respective neighboring boxes. In this paper we doc-

ument the steps which were taken to couple the TenStream solver to the UCLA-LES which permits us to drive atmospheric simulations with realistic 3D radiative heating rates.

Section 2 briefly introduces the TenStream solver and the UCLA-LES model. In section 2.2.1 follows a description of two choices of matrix solvers and preconditioners which primarily determine the performance of the TenStream solver.

In section 3 we repeated simulations according to the “Second Dynamics and Chemistry of Marine Stratocumulus field study” (DYCOMS II) to check the validity of the Monte-Carlo-Spectral-Integration. Section 4 presents an analysis of the weak- and strong-scaling behavior of the TenStream solver and section 5 discusses the applicability of the model setup for extended cloud-radiation interaction studies.

## 2 Description of models and core components

### 2.1 LES model

The LES that we coupled the TenStream solver to is the UCLA-LES model. A description and details of the LES model can be found in Stevens et al. (2005). The model already supports a 1D  $\delta$ -scaled four-stream solver to compute radiative heating rates. The spectral integration is performed following the correlated-k method of Fu and Liou (1992). We should briefly mention the changes to the model code which were necessary to support a three-dimensional solver.

In the case of three dimensional radiative transfer we need to solve the entire domain for one spectral band at once. This is in contrast to one dimensional radiative transfer solvers where the heating rate  $H(x, y, \lambda, z)$  is a function of the pixel  $(x, y)$ , integrated over spectral bands  $(\lambda)$  and solved for one vertical column  $(z)$  at a time. We therefore need to rearrange the loop structures from

$$H(x, y, \lambda, z) \rightarrow H(\lambda, x, y, z)$$

so that the spectral integration over  $\lambda$  is the outermost loop. The fact that we couple the entire domain, and hence need to select the same spectral band for all columns is different from what Pincus and Stevens (2009) did and may weaken the validity of the Monte-Carlo-Spectral-Integration. We will discuss this in section 3. The rearrangement also changes some vectors from 1D to 3D and may thereby introduce copies or caching issues. We find that the change roughly adds a 6 % speed penalty compared to the original single column code (no code optimizations considered). In this paper, calculations are exclusively done using the modified loop structures.

### 2.2 TenStream RT model

The TenStream radiative transfer model is a parallel approximate solver for the full 3D radiative transfer equation (Jakub and Mayer, 2015). In analogy to a two-stream solver, the

TenStream solver computes the radiative transfer coefficients for up- and downward fluxes and additionally for sideward streams. These transfer coefficients determine the propagation of energy through one box. The coupling of individual boxes ~~is done in~~ leads to a linear equation system which may be written as ~~sparse matrix and a~~ sparse matrix equation which is solved using parallel iterative methods. It is difficult to predict the performance of a specific choice of iterative solver or preconditioner beforehand. For that reason, we chose to use the “Portable, Extensible Toolkit for Scientific Computation”, PETSc (Balay et al., 2014) framework which offers a wide range of pluggable iterative solvers and matrix preconditioners. Jakub and Mayer (2015) found that the average increase in runtime compared to 1D two-stream solvers is about a factor of 15. One specifically interesting detail about the use of iterative solvers in the context of fluid dynamics simulations is the fact that we can use the solution at the last time step as an initial guess and thereby speed up the convergence of the solver. Section 4 presents detailed runtime comparisons on various computer architectures and simulation scenarios.

### 2.2.1 Matrix solver

The ~~resulting equation system of~~ coupling of radiative fluxes in the TenStream solver can be written as a huge but sparse matrix (i.e. most entries are zero). The TenStream matrix is positive definite (strictly diagonal dominant) and asymmetric. ~~Sparse Equation systems with~~ sparse matrices are usually solved using iterative methods because direct methods such as Gaussian-elimination or LU-factorization usually exceed memory limitations. The “Portable, Extensible Toolkit for Scientific Computation” (PETSc-Balay et al. (2014)) library includes several solvers and preconditioners to choose from.

### Iterative solvers

For three dimensional systems of partial differential equations with many degrees of freedom, iterative methods are often more efficient computationally and memory-wise. ~~It is also easier to implement them efficiently on today's compute hardware.~~ The three biggest classes in use today are Conjugate Gradient (CG), Generalized Minimal Residual Method (GMRES) and BiConjugate-Gradient methods (Saad, 2003). Given that CG is only suitable for symmetric matrices we will focus on the latter two. In the following we will use the flexible version of GMRES (Saad, 1993) and the “stabilized version of BiConjugate-Gradient-Squared” (Van der Vorst, 1992).

### Preconditioner

Perhaps even more important than the selection of a suitable solver is the choice of matrix preconditioning. In order to improve the rate of convergence, we try to find a transformation for the matrix that increases the efficiency of the main

iterative solver. We can use a preconditioner  $\mathcal{P}$  on the initial matrix equation so that it writes:

$$\mathcal{P}\mathcal{A} \cdot x = \mathcal{P}b$$

We can easily see that if  $\mathcal{P}$  is close to the inverse of  $\mathcal{A}$  the left hand side operator reduces to unity and the effort to solve the system is zero. Of course we cannot cheaply find the inverse of  $\mathcal{A}$  but we might find something that resembles  $\mathcal{A}^{-1}$  to a certain degree. Obviously for a good cost/efficiency tradeoff the preconditioner should be computationally cheap to apply and considerably reduce the number of iterations the solver needs to converge.

This study suggests two preconditioners for the TenStream solver. We are fully aware that our choices are probably not an optimal solution but they give reasonable results.

The first setup uses a so called stabilized BiConjugate-Gradient solver with incomplete LU factorization (ILU). Direct LU factorizations tend to fill up the ~~sparsity pattern~~ zero-entries (sparsity pattern) of the matrix and quickly become exceedingly expensive ~~memory-wise~~. A workaround is to only fill the preconditioner matrix until a certain threshold of filled entries are reached. A fill level factor of zero prescribes that the preconditioner matrix has the same number of non-zeros as the original matrix. The ILU preconditioner is only available sequentially and in the case of parallelized simulations, each processor applies the preconditioner independently (called “block-jacobi”). Consequently, the preconditioner can not propagate information beyond its local part and we will see in section 4 that this weakens the preconditioner for highly parallel simulations. ~~The solvers are commonly configured via command-line parameters (see listing 1 for ILU-preconditioning).~~

The second setup uses a flexible GMRES with geometric algebraic multigrid preconditioning (GAMG). Traditional iterative solvers like Gauss-Seidel or Block-Jacobi are very efficient in reducing ~~the high frequency error~~ local residuals at adjacent entries (often termed high frequency errors). This is why they are called “smoothers”. However, ~~the low frequency errors, i.e. long range~~ (low frequency) residuals, e.g. long range errors—a reflection at a distant location, are dampened only slowly. The general idea of multigrid is to solve the problem on several, coarser grids simultaneously. This way, the smoother is used optimally in the sense that on each grid representation the ~~error residual~~ which is targeted is rather high frequency error. This coarsening is done until ultimately the problem size is small enough to solve it with direct methods. Considerable effort has been put into the development of black-box multigrid preconditioners. Black-box means in this context that the user, in this case the TenStream solver, does not have to supply the coarse grid representation. Rather, the coarse grids are constructed directly from the matrix representation. The PETSc solvers are commonly configured via command-line ~~options to use parameters (see listing 1 for ILU-preconditioning or listing 2 for multigrid preconditioning are given in listing 2).~~



### 3 Monte Carlo Spectral Integration

There are two reasons why radiative transfer is so expensive computationally. On one hand, a single monochromatic calculation is already quite complex. On the other hand, radiative transfer calculations have to be integrated over a wide spectral range. Even if correlated-k methods are used, the number of radiative transfer calculations is on the order of a hundred. As a result, it becomes unacceptable to perform a full spectral integration at every dynamical time step, even with simple 1D two-stream solvers. This means that in most models, radiative transfer is performed at a lower rate than other physical processes. Pincus and Stevens (2009) proposed that instead of calculating radiative transfer spectrally dense and temporally sparse, one may sample only one spectral band at every model time step. The argument is that the error which is introduced by the coarse spectral sampling is averaged out over time and remains random and uncorrelated in space and time. As we mentioned in section 2.1, the three dimensional radiative transfer necessitates to compute the entire domain for one and the same spectral band instead of individual bands for each vertical column. In the following we will refer to the adapted version as uniform Monte-Carlo-Spectral-Integration. ~~It is not clear if the assumptions about the errors being random and uncorrelated still hold true if we reduce the sampling noise. To reason that the still holds true in the case of uniform spectral sampling, we~~ The uniform sampling relaxes the assumption that the errors are uncorrelated in space and it is therefore not clear whether it is still valid. We repeated the numerical experiment in close resemblance to the original paper of Pincus and Stevens (2009) and examine the results to validate the applicability of the uniform Monte-Carlo-Spectral-Integration.

There, they used the model setup for the DYCOMS-II simulation (details in Stevens et al. (2005)). They show results for nocturnal simulations. In contrast, here we show results with a constant zenith angle  $\theta = 45^\circ$ . Radiative transfer is computed with a 1D  $\delta$ -Eddington two-stream solver. The simulation is started with Monte-Carlo-Spectral-Integration and from 2.5 hours on, also calculated with the full spectral integration and the uniform Monte-Carlo-Spectral-Integration. Note, the good agreement between the full spectral sampling simulation and the one with the original Monte-Carlo-Spectral-Integration in fig. 1. The uniform formulation of Monte-Carlo-Spectral-Integration leads to high frequency changes in the average liquid water content (LWC). These fluctuation in LWC do however not lead to major differences in the evolution of the boundary layer clouds or turbulent kinetic energy. To put the changes in LWC into perspective, we ran the simulation again with ~~the a~~ a random perturbation on the boundary layer temperature field. The magnitude of the perturbation is chosen to be uniformly distributed between  $-5$  and  $5$  K and has a zero mean. We find that the temperature perturbation induces similar differences to the flow as does the Monte-Carlo-Spectral-

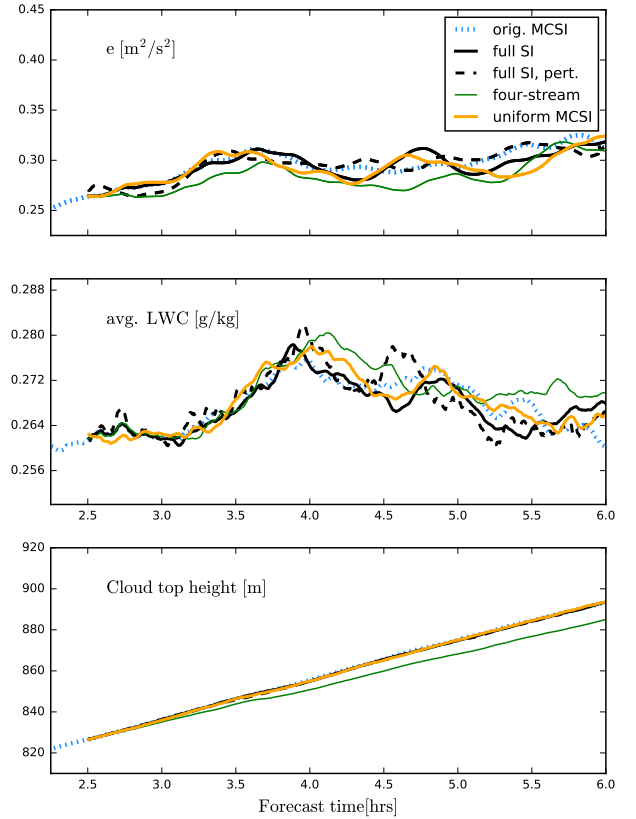


Figure 1: Intercomparison of the DYCOMS II simulation, once forced with the full radiation (solid line), with the original Monte-Carlo-Spectral-Integration (dotted) and with the uniform version (dashed). The dash-dotted line is a calculation with full spectral integration but with the four-stream solver instead of the two-stream solver. On the top panel, the vertically integrated turbulent kinetic energy, in the middle the mean liquid water content (conditionally sampled and weighted by physical height) and in the bottom panel the mean cloud top height.

Integration. Furthermore, we additional ran the simulation with the  $\delta$ -four-stream solver (Liou et al., 1988). While arguably both are good radiative transfer solvers, the choice of the solver leads to bigger ~~and biased changes differences~~ than the uniform Monte-Carlo-Spectral-Integration. The and even introduces a bias in the evolution of the cloud height. We therefore conclude, that while the uniform Monte-Carlo-Spectral-Integration may very well introduce considerable small scale errors but, it nevertheless seems to be a viable approximation for this type-kind of simulations. Additionally, we repeated the same kind of experiment for several other scenarios (broken cumulus and deep convection), all confirming the applicability of the uniform Monte-Carlo-Spectral-Integration.

## 4 Performance Statistics

To determine the parallel scaling behavior when using an increasing number of processors, one usually conducts two experiments: First, a so called “strong-scaling” experiment where the problem size stays constant while the number of processors is gradually increased. We speak of linear strong-scaling behavior if the time needed to solve the problem is reduced proportional to the number of used processors. Secondly, a “weak-scaling” experiment where the problem size and the number of processors are increased linearly, i.e. the workload per processor is fixed. Linear weak-scaling efficiency implies that the time-to-solution remains constant.

### 4.1 Strong scaling

We hypothesized earlier (section 2.2) that a good initial guess for the iterative solver results in a faster convergence rate. To test this assumption we performed two strong scaling (problem size stays the same) simulations. One “clear-sky” experiment without clouds in which the difference between radiation calls is minimal and a “warm-bubble” case with a strong cloud deformation and displacement in between time steps. These two situations enclose what the solver may be used for and are hence the extreme cases with respect to the computational effort.

Both scenarios have principally the same setup with a domain length of 10 km at a horizontal resolution of 100 m. The model domain is divided into 50 vertical layers with 70 m resolution at the surface and a vertical grid stretching of 2 %. The atmosphere is moist and neutrally stable (see section 6 for namelist parameters). Simulations are performed with warm cloud microphysics, a constant surface temperature, without Monte-Carlo-Spectral-Integration and a dynamic timestep of about 2 s.

Both scenarios are run forward in time for an hour for different solar zenith angles and with varying matrix solvers and preconditioners (presented in section 2.2.1). The difference between the first and the second simulation is the external forcing that was applied. The “clear-sky”-case is initialized with less moisture, weaker initial wind and no temperature perturbation. No clouds develop in the course of the simulation. In contrast, the second case is initialized with a saturated moisture profile, a strong wind field and a positive, bell shaped, temperature perturbation in the lower atmosphere. The temperature perturbation leads to a rising warm bubble which leads to a cloud shortly after. The initial forcing and latent heat release leads to strong updrafts up to  $19 \text{ m s}^{-1}$  while the horizontal wind with up to  $15 \text{ m s}^{-1}$  quickly displaces the cloud sideways. This strong deformation should give an upper bound on the dissimilarity between calls to the radiation scheme and therefore reduce the quality of the initial guess. To illustrate the general behavior of the strong- and weak scaling experiments, fig. 2 depicts the warm bubble simulation (for the purpose of visualization without initial

horizontal wind) – once driven by 1D radiative transfer and once more with the TenStream solver.

Figure 3 presents the increase in runtime of the TenStream solver compared to a 1D calculation. All timings are taken as a best of three and simulations were performed on the IBM Power6 “Blizzard” at DKRZ (Deutsches Klimarechenzentrum), Hamburg in SMT mode<sup>1</sup>. To solve for the direct and diffuse fluxes, the matrix coefficients for the radiation propagation (stored in a 6-dim look-up table) need to be determined for given local optical properties. Retrieving the transport coefficients from the look-up table and the respective linear interpolation (green bar) takes about as long as the 1D radiative transfer calculation alone and is expectedly independent of parallelization and the initial guess of the solution. For larger zenith angles, i.e. lower sun angles, the calculation of direct radiation becomes more and more expensive because of the increasing communication between processors. Note that the computational effort also increases in case of single core runs – the iterative solver needs more iterations because of its treatment of cyclic boundary conditions. The “clear-sky” simulations are computationally cheaper than the more challenging cloud producing “warm-bubble” simulations. In the former, the solver often converges in just one iteration where as in the latter, rather complex case, more iterations are needed. Note that the ILU preconditioning weakens if more processors are used. The ILU is a serial preconditioner and in the case of parallel computations, it is applied to each sub-domain independently. The ILU-preconditioner hence can not propagate information between processors.

The performance of Multi-Grid preconditioning (GAMG) is less affected by parallelization. The number of iterations until converged stays close to constant (independent of the number of processors). The GAMG preconditioning outperforms the ILU preconditioning for many-core systems whereas the setup cost of the coarse grids as well as the interpolation and restriction operators are more expensive if the problem is solved on a few cores only. In summary, we expect the increase in runtime compared to traditionally employed 1D two-stream solvers to be in the range between five to ten times.

### 4.2 Weak scaling

We examine the weak-scaling behavior using the earlier presented simulation (see section 4.1) but run it only for 10 min. The experiment uses multigrid preconditioning and only performs calculations in the thermal spectral range. The number of grid points is chosen to be 16 by 16 per MPI-rank ( $\approx 10^5$  unknown fluxes or  $\approx 10^6$  transfer coefficients per processor). The simulations were performed at three different machines/networks (see table 1). Please note that the simulations for Mistral (see table 1) do not fill up the entire nodes (24

<sup>1</sup>SMT – Simultaneous Multithreading (2 ranks/core)



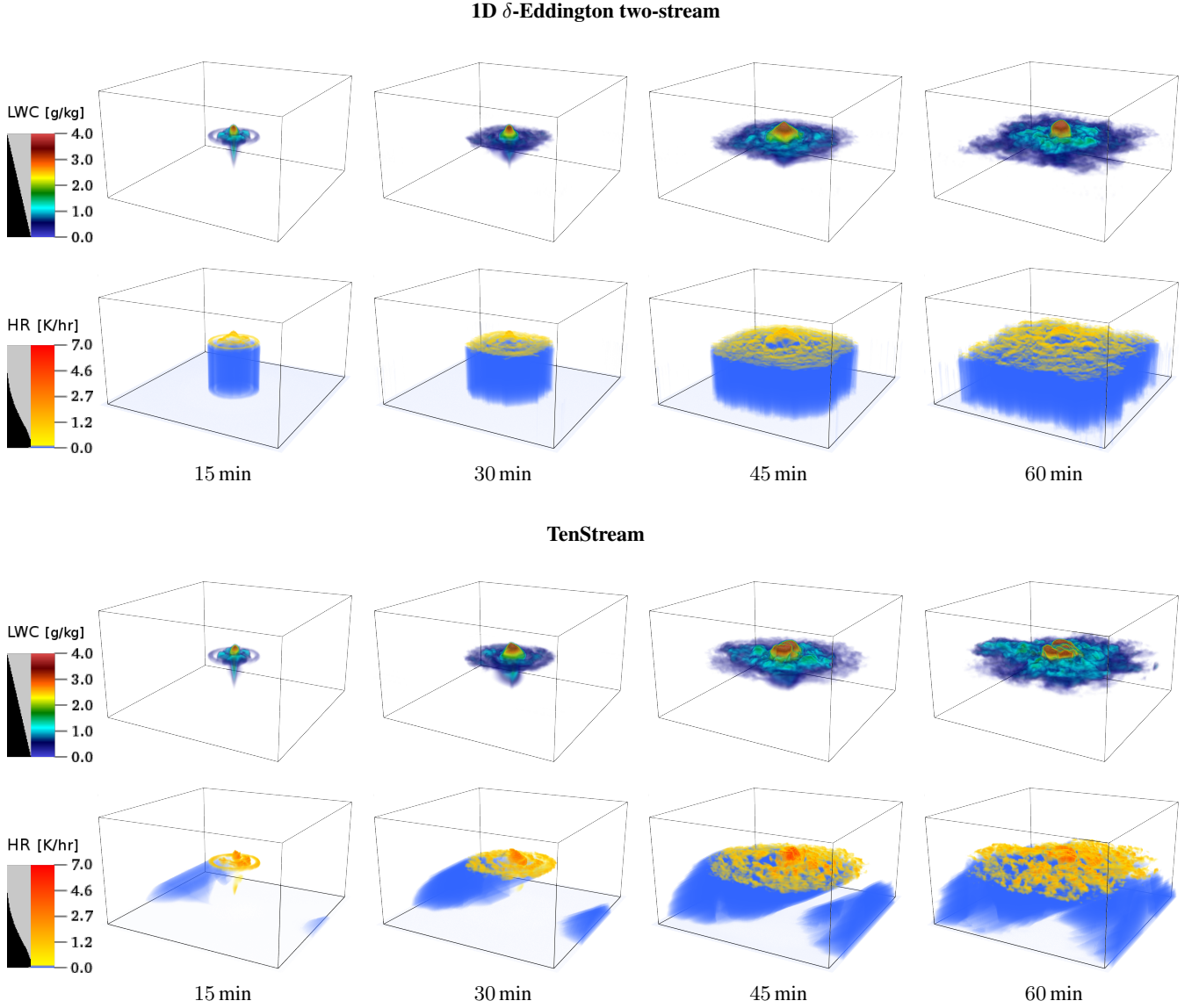


Figure 2: Volume rendered perspective on liquid water content and solar atmospheric heating rates of the warm-bubble experiment (initialized without horizontal wind). The two upper panels depict a simulation which was driven by 1D radiative transfer and the two lower panels show a simulation where radiative transfer is computed with the TenStream solver ( solar zenith angle  $\theta = 60^\circ$ ; const. surface fluxes). Three-dimensional effects in atmospheric heating rates introduce anisotropy which in turn has a feedback on cloud evolution. Domain dimensions are  $12.8 \text{ km} \times 12.8 \text{ km}$  horizontally and  $5 \text{ km}$  vertically at a resolution of  $50 \text{ m}$  in each direction. See section 6 for simulation parameters. Gray bar in the legend **represents the alpha channel and** determines the transparency of the individual colors for the volume renderer.

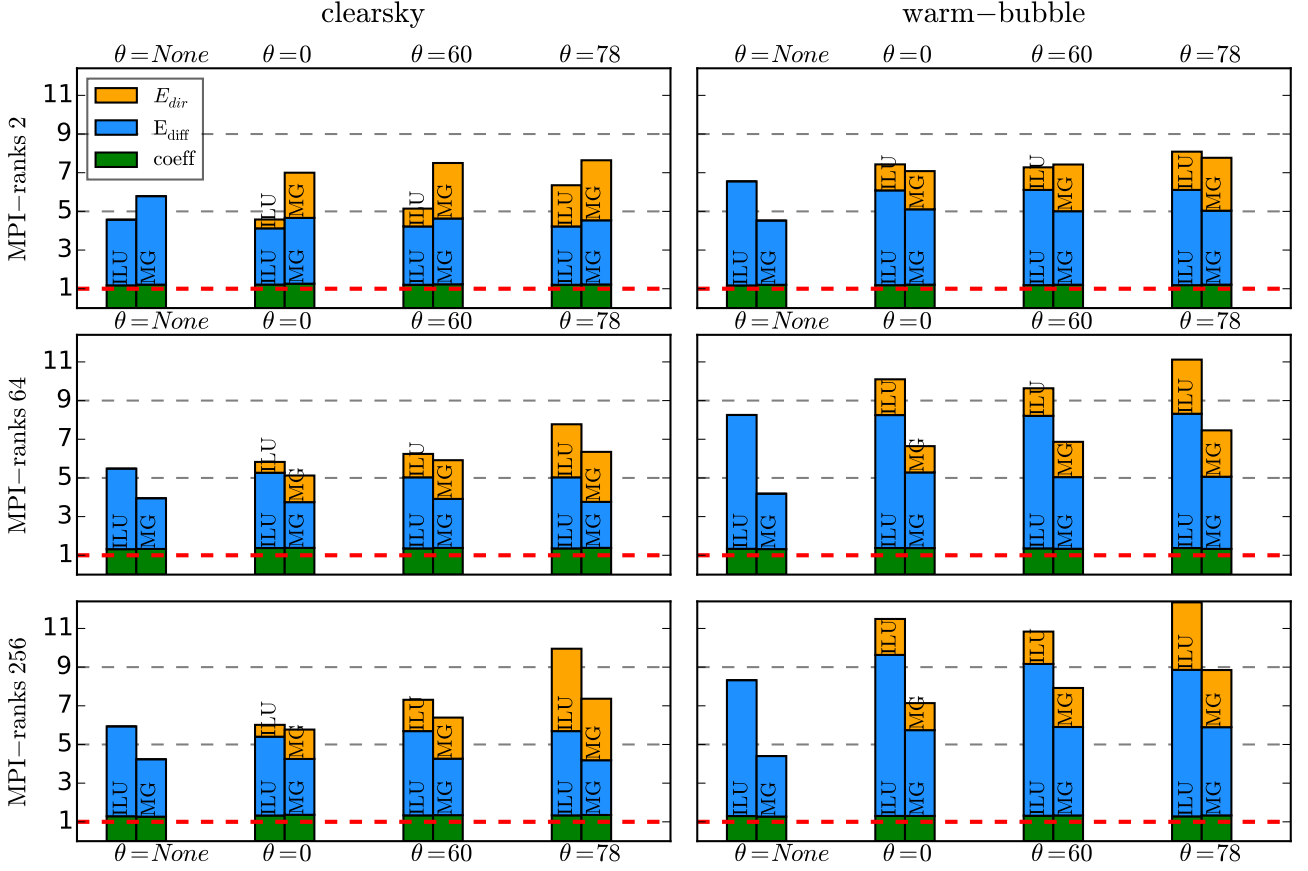


Figure 3: Two strong scaling tests for a clear-sky and a strongly forced scenario. Vertical axis is the increase of computational time normalized to a delta-eddington two-stream calculation (solvers only). Horizontal axis is for different solar zenith angles ( $\theta = \text{None}$  means thermal only, no solar radiation). The stacked bars denoting time used for the individual components of the solver. “Coeff” meaning the time needed to retrieve and interpolate the transport coefficients.  $E_{\text{diff}}$  is the elapsed time that was used to set up the source term and solve for the diffuse radiation; the same for the direct radiation in  $E_{\text{dir}}$ . The bars are labeled with the corresponding matrix preconditioning.

	Ranks / Node	Cores	Memory- Bandwidth
Mistral	24	2x12@2.5 GHz	112 GB s <sup>-1</sup>
Blizzard	64	4x 8@4.7 GHz	37 GB s <sup>-1</sup>
Thunder	16	2x 8@2.6 GHz	76 GB s <sup>-1</sup>

Table 1: Details on the computers used in this work. Mistral and Blizzard are Intel-Haswell and IBM Power6 supercomputers at DKRZ, Hamburg, respectively. Thunder denotes a Linux Cluster at ZMAW, Hamburg. Columns are the number of MPI ranks used per compute node, the number of sockets and cores, and the maximum memory-bandwidth per node as measured by the streams (McCalpin, 1995) benchmark.

cores) since UCLA-LES can currently only run on a number of cores which is a power of two.

Figure 4 presents the weak-scaling efficiency  $f$ , defined by:

$$f = \frac{t_{\text{single core}}}{t_{\text{multi core}}} \cdot 100\%$$

The scaling behavior can be separated into two regimes: the efficiency on one compute node and the efficiency of the network communication. As long as we stick to one node (fig. 4a), the loss of scaling concerns the 3D TenStream solver as well as the 1D two-stream solver. Reasons for the reduced efficiency may be cache-issues, hyper-threading or memory-bus saturation. The scaling behavior for more than one node (fig. 4b) shows a close to linear scaling for the 1D two-stream solver and a decrease in performance in the case of the TenStream solver. The limiting factor here is network latency and throughput.

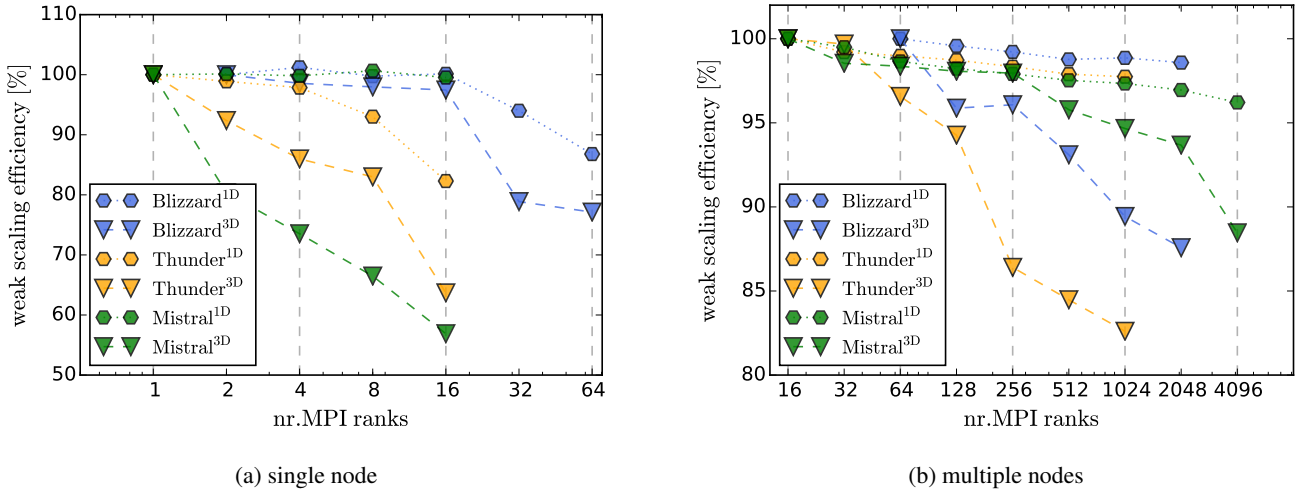


Figure 4: Weak scaling efficiency running UCLA-LES with interactive radiation schemes. Experiments measure the time for the radiation solvers only (i.e. no dynamics or computation of optical properties). Timings are given as a best of 10 runs. Weak scaling efficiency is given for the TenStream solver (triangle markers) as well as for a two-stream solver (hexagonal markers). (Left) scaling behavior compared to single core computations (remaining on one compute node). (Right) Compute node parallel scaling (normalized against a single node). The individually colored lines correspond to different machines (see table 1 for details) and calculations once done with the  $\delta$ -eddington two-stream solver (hexagons) and once with the TenStream solver (triangles).

## 5 Conclusions

We described the necessary steps to couple the 3D TenStream radiation solver to the UCLA-LES model. From a technical perspective, this involved the reorganization of the loop structure, i.e. first calculate the optical properties for the entire domain and then solve the radiative transfer.

It was not obvious that the Monte-Carlo-Spectral-Integration would still be valid for 3D radiative transfer. To that end, we conducted numerical experiments (DYCOMS II) in close resemblance to the work of Pincus and Stevens (2009) and find that the Monte-Carlo-Spectral-Integration holds true, even in case of horizontally coupled radiative transfer where the same spectral band is used for the entire domain.

The convergence rate of iterative solvers is highly dependent on the applied matrix-preconditioner. In this work, we tested two different matrix-preconditioners for the TenStream solver: First, an incomplete LU decomposition and secondly the algebraic multigrid-preconditioner, GAMG. We found that the GAMG preconditioning is superior to the ILU in most cases and especially so for highly parallel simulations.

The increase in runtime is dependent on the complexity of the simulation (how much the atmosphere changes between radiation calls) and the solar zenith angle. We evaluated the performance of the TenStream solver in a weak and strong scaling experiment and presented runtime comparisons to a

1D  $\delta$ -eddington two-stream solver. The increase in runtime for the radiation calculations ranges from a factor of five up to ten. The total runtime of the LES simulation increased roughly by a factor of two to three. A only twofold increase in runtime allows extensive studies concerning the impact of three dimensional radiative heating on cloud evolution and organization.

This study aimed at documenting the performance and applicability of the TenStream solver in the context of high-resolution modeling. Subsequent work has to quantify the impact of three dimensional radiative heating rates on the dynamics of the model.

## 6 Code availability

The UCLA-LES model is publicly available at <https://github.com/uclales>. The calculations were done with the modified radiation interface which is available at git-revision “bbcc4e08ed4cc0789b33e9f2165ac63a7d0573ef”.

To obtain a copy of the TenStream code, please contact one of the authors. This study used the TenStream model at git-revision “e0252dd9591579d7bfb8f374ca3b3e6ce9788cd2”. For the sake of reproducibility we provide the input parameters for the here mentioned UCLA-LES computations along with the TenStream sources.

## Appendix A: Input parameters for the PETSc solvers

Listing 1: BiConjugate-Gradient-Squared iterative solver. The block-jacobi preconditioner does a Incomplete LU preconditioning on each rank with fill level 1 independent of its neighbouring ranks

```
-ksp_type bcgs
-pc_type bjacobi
-sub_pc_type ilu
-sub_pc_factor_levels 1
```

Listing 2: Flexible GMRES solver with algebraic multigrid preconditioning. Use plain aggregation to generate coarse representation (dropping values less than .1 to reduce coarse matrix complexity) and use up to 5 iterations of SOR on coarse grids

```
-ksp_type fgmres
-ksp_reuse_preconditioner
-pc_type gamg
-pc_gamg_type agg
-pc_gamg_agg_nsmooths 0
-pc_gamg_threshold .1
-pc_gamg_square_graph 1
-mg_levels_ksp_type richardson
-mg_levels_pc_type sor
-mg_levels_ksp_max_it 5
```

*Acknowledgements.* This work was funded by the Federal Ministry of Education and Research (BMBF) through the High Definition Clouds and Precipitation for Climate Prediction (HD(CP)2) project (FKZ: 01LK1208A). Many thanks to Bjorn Stevens and the DKRZ, Hamburg for providing us with the computational resources to conduct our studies.

## References

- Balay, S., Abhyankar, S., Adams, M. F., Brown, J., Brune, P., Buschelman, K., Eijkhout, V., Gropp, W. D., Kaushik, D., Knepley, M. G., McInnes, L. C., Rupp, K., Smith, B. F., and Zhang, H.: PETSc Users Manual, Tech. Rep. ANL-95/11 - Revision 3.5, Argonne National Laboratory, 2014.
- Di Giuseppe, F. and Tompkins, A.: Three-dimensional radiative transfer in tropical deep convective clouds, *Journal of Geophysical Research: Atmospheres* (1984–2012), 108, doi:10.1029/2003JD003392, 2003.
- Evans, K. F.: The spherical harmonics discrete ordinate method for three-dimensional atmospheric radiative transfer, *Journal of the Atmospheric Sciences*, 55, 429–446, doi:10.1175/1520-0469(1998)055<0429:TSHDOM>2.0.CO;2, 1998.
- Frame, J. W., Petters, J. L., Markowski, P. M., and Harrington, J. Y.: An application of the tilted independent pixel approximation to cumulonimbus environments, *Atmospheric Research*, 91, 127–136, doi:10.1016/j.atmosres.2008.05.005, 2009.
- Fu, Q. and Liou, K.: On the correlated k-distribution method for radiative transfer in nonhomogeneous atmospheres, *Journal of the Atmospheric Sciences*, 49, 2139–2156, doi:10.1175/1520-0469(1992)049<2139:OTCDMF>2.0.CO;2, 1992.
- Harrington, J. Y., Feingold, G., and Cotton, W. R.: Radiative impacts on the growth of a population of drops within simulated summertime arctic stratus, *Journal of the atmospheric sciences*, 57, 766–785, doi:10.1175/1520-0469(2000)057<0766:RIOTGO>2.0.CO;2, 2000.
- Hogan, R. J. and Shonk, J. K.: Incorporating the effects of 3D radiative transfer in the presence of clouds into two-stream multilayer radiation schemes, *Journal of the Atmospheric Sciences*, 70, 708–724, 2013.
- Jakub, F. and Mayer, B.: A three-dimensional parallel radiative transfer model for atmospheric heating rates for use in cloud resolving models—The TenStream solver, *Journal of Quantitative Spectroscopy and Radiative Transfer*, pp. –, doi:http://dx.doi.org/10.1016/j.jqsrt.2015.05.003, <http://www.sciencedirect.com/science/article/pii/S0022407315001727>, 2015.
- Joseph, J., Wiscombe, W., and Weinman, J.: The Delta-Eddington approximation for radiative flux transfer, *J. Atmos. Sci.*, 33, 2452–2459, doi:10.1175/1520-0469(1976)033<2452:TDEAFR>2.0.CO;2, 1976.
- Klinger, C. and Mayer, B.: The Neighbouring Column Approximation (NCA)—A fast approach for the calculation of 3D thermal heating rates in cloud resolving models, *Journal of Quantitative Spectroscopy and Radiative Transfer*, doi:doi:10.1016/j.jqsrt.2015.08.020, 2015.
- Liou, K.-N., Fu, Q., and Ackerman, T. P.: A simple formulation of the delta-four-stream approximation for radiative transfer parameterizations, *Journal of the atmospheric sciences*, 45, 1940–1948, 1988.
- Marquis, J. and Harrington, J. Y.: Radiative influences on drop and cloud condensation nuclei equilibrium in stratocumulus, *Journal of Geophysical Research: Atmospheres* (1984–2012), 110, doi:10.1029/2004JD005401, 2005.
- Mayer, B.: Radiative transfer in the cloudy atmosphere, in: *EPJ Web of Conferences*, vol. 1, pp. 75–99, EDP Sciences, doi:10.1140/epjconf/e2009-00912-1, 2009.
- McCalpin, J. D.: Memory Bandwidth and Machine Balance in Current High Performance Computers, *IEEE Computer Society Technical Committee on Computer Architecture (TCCA) Newsletter*, pp. 19–25, 1995.
- Mlawer, E. J., Taubman, S. J., Brown, P. D., Iacono, M. J., and Clough, S. A.: Radiative transfer for inhomogeneous atmospheres: RRTM, a validated correlated-k model for the longwave, *Journal of Geophysical Research: Atmospheres* (1984–2012), 102, 16 663–16 682, doi:10.1029/97JD00237, 1997.
- Muller, C. and Bony, S.: What favors convective aggregation and why?, *Geophysical Research Letters*, 42, 5626–5634, doi:10.1002/2015GL064260, 2015.
- O’Hirok, W. and Gautier, C.: The impact of model resolution on differences between independent column approximation and Monte Carlo estimates of shortwave surface irradiance and atmospheric heating rate., *Journal of the atmospheric sciences*, 62, doi:10.1175/JAS3519.1, 2005.
- Petters, J. L.: The impact of radiative heating and cooling on marine stratocumulus dynamics, 2009.
- Pincus, R. and Stevens, B.: Monte Carlo spectral integration: A consistent approximation for radiative transfer in large eddy sim-

- 595     ulations, *Journal of Advances in Modeling Earth Systems*, 1,  
      doi:10.3894/JAMES.2009.1.1, 2009.
- Saad, Y.: A flexible inner-outer preconditioned GMRES algorithm,  
      *SIAM Journal on Scientific Computing*, 14, 461–469, 1993.
- Saad, Y.: *Iterative methods for sparse linear systems*, Siam, 2003.
- 600     Schumann, U., Dörnbrack, A., and Mayer, B.: Cloud-shadow effects  
      on the structure of the convective boundary layer, *Meteorologis-*  
      *che Zeitschrift*, 11, 285–294, 2002.
- Stevens, B., Moeng, C.-H., Ackerman, A. S., Bretherton, C. S.,  
      Chlond, A., de Roode, S., Edwards, J., Golaz, J.-C., Jiang, H.,  
605     Khairoutdinov, M., et al.: Evaluation of large-eddy simulations  
      via observations of nocturnal marine stratocumulus, *Monthly*  
      *weather review*, 133, 1443–1462, doi:10.1175/MWR2930.1,  
      2005.
- Tompkins, A. M. and Di Giuseppe, F.: Generalizing cloud overlap  
610     treatment to include solar zenith angle effects on cloud geometry,  
      *Journal of the atmospheric sciences*, 64, 2116–2125, 2007.
- Van der Vorst, H. A.: Bi-CGSTAB: A fast and smoothly converging  
      variant of Bi-CG for the solution of nonsymmetric linear sys-  
      tems, *SIAM Journal on scientific and Statistical Computing*, 13,  
615     631–644, doi:10.1137/0913035, 1992.
- Wissmeier, U., Buras, R., and Mayer, B.: paNTICA: A Fast 3D Ra-  
      diative Transfer Scheme to Calculate Surface Solar Irradiance for  
      NWP and LES Models., *Journal of Applied Meteorology & Cli-*  
      *matology*, 52, doi:10.1175/JAMC-D-12-0227.1, 2013.